Synthesis, Structure, Magnetism and Electrochemistry of Binuclear Nickel(II) and Copper(II) Complexes of an Unsymmetrical Pentadentate Schiff-base Ligand†

Paul E. Kruger,[a] Boujemaa Moubaraki,[a] Keith S. Murray*,[a] and Edward R. T. Tiekink[b]
[a] *Department of Chemistry, Monash University, Clayton, Victoria 3168, Australia*
[b] *Department of Physical and Inorganic Chemistry, University of Adelaide, South Australia 5001, Australia*

A new unsymmetrical binucleating ligand, H_3L, containing salicylidene and 1-methyl-3-oxobut-1-enyl end groups attached to a 1,3-diaminopropan-2-ol backbone, has been synthesized. Binuclear nickel(II) and copper(II) complexes of this ligand, of the type $[M_2L(pz)]$, containing a μ-pyrazolato (pz) exogenous bridging group and a μ-alkoxo endogenous bridge, have been synthesized and characterized. Cyclic voltammetric studies on dimethylformamide solutions of these complexes revealed well resolved waves attributable to sequential one-electron metal-centred reduction processes to yield the species $[M_2L(pz)]^-$ and $[M_2L(pz)]^{2-}$. Comparison to published electrochemical data on the compounds of analogous symmetrical ligands allows identification of the metal–salicylidene end as the site of the first electron transfer. Magnetic susceptibility studies on powdered samples of $[Cu_2L(pz)]$ show medium-strength antiferromagnetic coupling ($J_{12} = -129$ cm^{-1}) within the binuclear molecules and weaker antiferromagnetic coupling ($J_{\text{intermol}} = -41$ cm^{-1}) between the molecules. Intermolecular Ni···Ni contact distances of 3.442(5) and 5.100(4) Å are evident in the crystal packing of $[Ni_2L(pz)]$. Crystals of the latter have $Z = 2$ in a triclinic cell with space group $P\bar{1}$ and dimensions $a = 9.084(2)$, $b = 12.185(4)$, $c = 8.269(1)$ Å, $\alpha = 98.01(2)$, $\beta = 100.55(1)$, $\gamma = 99.03(2)$°; $R = 0.087$ based on 1283 reflections with $I \geqslant 3.0\sigma(I)$. The structure shows each nickel(II) ion to have a square-planar *trans*-N_2O_2 environment and the whole binuclear molecule to be essentially planar. The Ni(1)···Ni(2) distance is 3.212(4) Å.

The field of binucleating ligands and their metal complexes has developed considerably in recent years.[1,2] This is partly because of the interest in relating structures to magnetic exchange effects in homo- and hetero-binuclear metal complexes of these ligands[3-5] and partly because of the use of such complexes to mimic aspects of two-metal biosites in various proteins and enzymes.[6,7] In the latter context the reactivity of such complexes towards substrates such as dioxygen[6] and the redox properties in general[8] are of equal importance to magneto-structural correlations. One design feature which is of particular relevance, not only to mimicking the structures of certain two-metal active sites (*e.g.*, Fe_2 sites in haemerythrin[7]), but also to the ability of such ligands to form hetero- rather than homo-binuclear complexes, is a lack of symmetry relative to the centre of the ligand. This can be seen in the schematic structure **1** of a binuclear complex of general type $[M_2(\text{ligand})X]$ which contains different end-group donor sets, Z,Z and Z′,Z′, on opposite sides of the endogenous (Y)–exogenous (X) bridging atom axis, *a*. The few known examples which display a lack of symmetry across *a* include complexes of compartmental ligands having phenolate or enolate endogenous atoms shown in **3**[3] and **4**.[9] However, both of these structures are symmetrical across the M···M axis. In the present case we have extended our earlier studies on Schiff-base complexes of type **2**,[10,11] which are structurally symmetrical on each side of *a* but unsymmetrical relative to the M···M axis, into a molecular design of type **1**, shown in **5**, which is unsymmetrical in both directions. The new pentadentate compound H_3L contains salicylideneimine and acetylacetone imine end groups attached to a propan-2-ol backbone. Its synthesis involved the use of the new amine precursor **I**. The spectroscopic, magnetic and electrochemical properties of the homobinuclear species $[M_2L(pz)]$ are described, where M^{II} = Ni or Cu and pz = pyrazolate. The crystal structure of $[Ni_2L(pz)]$ is also briefly described.

We note that other groups are presently investigating unsymmetrical complexes of type **1** containing different end groups and backbone fragments to those used here.[12-16] We, and others, have also recently obtained unsymmetrical homobinuclear species, in some cases by chance, the lack of symmetry in such cases being brought about by factors such as differences in axial ligation and in donor-atom arrangement around each metal ion.[17-20]

Experimental

CAUTION: Perchlorate salts are potentially explosive and should only be handled in small quantities.

Materials.—All chemicals and solvents used were of reagent grade. Solvents used for physical measurements were of spectroscopic grade. The compounds $Cu(ClO_4)_2\cdot6H_2O$, $Ni(ClO_4)_2\cdot6H_2O$, pyrazole, 3,5-dimethylpyrazole and 1,3-diaminopropan-2-ol were obtained from Aldrich Chemical Co. Acetylacetone was obtained from Hopkin and Williams Ltd., salicylaldehyde from Riedel-de-Haën.

Synthesis of 1-(1-*Methyl*-3-*oxobut*-1-*enylamino*)-3-(*salicylideneamino*)*propan*-2-*ol*, H_3L.—A chloroform solution (50 cm^3) containing freshly distilled acetylacetone (5.01 g, 0.05 mol) was added dropwise to a vigorously stirred chloroform solution of 1,3-diaminopropan-2-ol (4.44 g, 0.05 mol) over a period of 30 min. After the addition was complete the solution was allowed to stand at ambient temperature for 8 h, after which time the solvent was removed under reduced pressure to retrieve a viscous yellow oil or a milky yellow slurry. This intermediate,

---

† *Supplementary data available:* see Instructions for Authors, *J. Chem. Soc., Dalton Trans.*, 1994, Issue 1, pp. xxiii–xxviii.
Non-SI unit employed: $\mu_B \approx 9.274 \times 10^{-24}$ J T^{-1}.

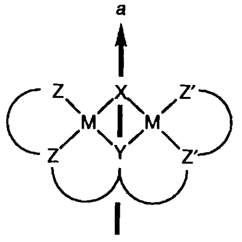

1

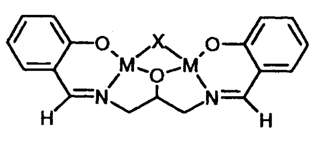

2

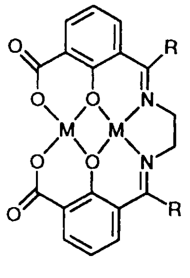

3

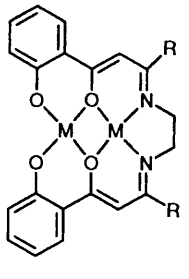

4

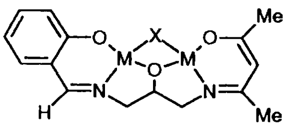

5

$[M_2L(X)]$

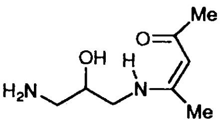

I

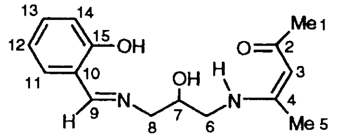

H_3L

I, was then used directly in the subsequent step. The residue was dissolved in methanol (50 cm^3), warmed slightly and to this was added, with stirring, a stoichiometric amount of salicylaldehyde. After the full development of a golden yellow solution, evaporation of the solvent yielded a pale yellow crystalline solid which was extracted into chloroform (150 cm^3) and washed three times with distilled water. The organic phase was dried with $MgSO_4$, filtered and its volume reduced. Crystallization was induced through the addition of ice-cold diethyl ether. The resulting pale yellow solid was collected and dried under high vacuum. Several more crops were obtained from the filtrate on standing. Total yield $\approx 70\%$. M.p. 116–117 °C. IR (Nujol, cm^{-1}): 3270s, 1635s, 1607s, 1564s, 1525m, 1499w, 1331m, 1305s, 1275s, 1213w, 1148w, 1084w, 1054w, 1022w, 972w, 958m, 945m, 884w, 779m, 759s, 738w, 720m and 706w. UV/VIS spectrum ($CHCl_3$): λ/nm (ε/dm^3 mol^{-1} cm^{-1}) 258 (10 601), 314 (24 924) and 415 (82). NMR ($CDCl_3$): ^1H (300 MHz), δ 13.2 (br s, 1 H, ex), 10.9 (br t, 1 H, ex), 8.4 (s, 1 H, imine), 7.4–7.2 (m, 2 H, phenyl), 6.9–6.7 (m, 2 H, phenyl), 4.9 (s, 1 H, methine), 4.1 (m, 1 H, CHO), 3.7 (m, 2 H, CH_2), 3.4 (m, 2 H, CH_2), 1.95 (s, 3 H, CH_3) and 1.90 (s, 3 H, CH_3); ^{13}C (75 MHz), δ 194 (C^2), 167 (C^9), 163 (C^4), 161 (C^{15}), 132.4 (C^{13}), 131.5 (C^{11}), 120 (C^{10}), 118.6 (C^{12}), 116.7 (C^{14}), 95.8 (C^3), 69.7 (C^7), 62.7 (C^8), 46.8 (C^6), 28.5 (C^1) and 19.0 (C^5). Mass spectrum: m/z 276, M^+.

Synthesis of the Complexes $[Ni_2L(pz)]$ *and* $[Cu_2L(pz)]$.—To a methanolic solution containing H_3L, pyrazole (Hpz) and the respective metal perchlorate was added, with vigorous stirring, a methanolic solution of KOH (1 : 1 : 2 : 4) resulting in the formation of either a red-brown (Ni) or violet (Cu) slurry. The mixture was filtered to remove the solids and allowed to dry. Recrystallization was achieved by Soxhlet extraction over several hours using CH_2Cl_2–$CHCl_3$. Microcrystalline compounds were obtained by slow evaporation of the solvent. The 3,5-dimethylpyrazolate (dmpz) analogue was prepared in an identical manner to the above except dimethylpyrazole was used in place of pyrazole.

$[Ni_2L(pz)]$ (Found: C, 47.2; H, 4.5; N, 12.1. Calc. for $C_{18}H_{20}N_4Ni_2O_3$: C, 47.2; H, 4.4; N, 12.2%). UV/VIS spectrum ($CHCl_3$): λ/nm (ε/dm^3 mol^{-1} cm^{-1}) 350 (3150), 418 (1223) and 451 (808). NMR ($CDCl_3$): ^1H (300 MHz), δ 7.4 (s, 1 H, imine), 7.2–6.9 (m, 4 H, phenyl), 6.75 (d, 1 H, pz), 6.4 (t, 1 H, pz), 5.9 (d, 1 H, pz), 4.75 (s, 1 H, methine), 4.1 (m, 1 H, CHO), 3.3 (t, 1 H, CH_2), 3.0 (dd, 1 H, CH_2), 2.75 (m, 2 H, CH_2), 1.8 (s, 3 H, CH_3) and 1.7 (s, 3 H, CH_3); ^{13}C (75 MHz), δ 178 (C^2), 164.6 (C^4), 164.1 (C^{15}), 161 (C^9), 136.5 (C^{16}, pz), 136.4 (C^{18}, pz), 133.3 (C^{13}), 132.6 (C^{11}), 121.5 (C^{12}), 120.7 (C^{10}), 114.8 (C^{14}), 102.7 (C^{17}, pz), 99.7 (C^3), 78.5 (C^7), 61.2 (C^8), 54.5 (C^6), 24.0 (C^1) and 20.6 (C^5).

$[Ni_2L(dmpz)]$ (Found: C, 49.6; H, 5.1; N, 11.7. Calc. for $C_{20}H_{24}N_4Ni_2O_3$: C, 49.6; H, 5.0; N, 11.6%). NMR ($CDCl_3$): ^1H (300 MHz), δ 7.4 (s, 1 H, imine), 7.3–7.1 (m, 2 H, phenyl), 6.8–6.7 (m, 1 H, phenyl), 6.6–6.5 (m, 1 H, phenyl), 5.4 (s, 1 H, pz), 4.9 (s, 1 H, methine), 3.5 (m, 1 H, CHO), 3.3 (m, 1 H, CH_2), 3.1 (m, 2 H, CH_2), 2.7 (m, 1 H, CH_2), 2.15 (s, 3 H, CH_3 of dmpz), 2.05 (s, 3 H, CH_3 of dmpz), 1.9 (s, 3 H, CH_3) and 1.7 (s, 3 H, CH_3); ^{13}C (75 MHz), δ 176 (C^2), 164.4 (C^4), 164.1 (C^{15}), 160.4 (C^9), 149.8–149.7 (C^{16}, C^{18}, dmpz), 133.3 (C^{13}), 132.1 (C^{11}), 120.8 (C^{12}), 120.5 (C^{10}), 114.8 (C^{14}), 107 (C^{17}, dmpz), 100 (C^3), 74 (C^7), 63.6 (C^8), 56.2 (C^6), 23.2 (C^1), 20.4 (C^5) and 12.6–12.5 (CH_3 of dmpz).

$[Cu_2L(pz)]$ (Found: C, 46.3; H, 4.4; N, 12.0. Calc. for $C_{18}H_{20}Cu_2N_4O_3$: C, 46.2; H, 4.3; N, 12.0%). UV/VIS spectrum ($CHCl_3$): λ/nm (ε/dm^3 mol^{-1} cm^{-1}) 318 (6240), 370 (3200) and 569 (320). μ_{eff} 1.33 μ_B per Cu at 295 K.

Physical Methods.—Infrared spectra were measured on a Perkin-Elmer 1600 FT-IR instrument with the samples as Nujol mulls or KBr pellets. Abbreviations used: s = strong; m = medium; w = weak; sh = shoulder; br = broad. Chemical analyses, C, H, N, were performed by the Commonwealth Micro-analytical Services, Melbourne, Australia. Melting points were determined on an Electrothermal IA6304 apparatus and are uncorrected. Ultraviolet–visible spectra were recorded on a Hitachi 150–20 spectrophotometer using 1 cm quartz cells and solution concentrations of 10^{-4} mol dm^{-3}. Magnetic moments at room temperature were determined using a Faraday balance which incorporated a Newport electromagnet fitted with Faraday-profile pole faces. The instrument was calibrated using $[Ni(en)_3][S_2O_3]$ (en = ethane-1,2-diamine) and $CuSO_4 \cdot 5H_2O$. Diamagnetic corrections for ligand susceptibilities were made using Pascal's constants. Variable-temperature magnetic susceptibility measurements (300–4.2 K) were performed on powdered samples at a field strength of 10 000 G (1 T) using a Quantum Design M.P.M.S. Squid magnetometer. The calibration of the instrument was checked regularly against samples of pure palladium and AR $CuSO_4 \cdot 5H_2O$. Samples were enclosed in gelatin capsules suspended at the middle of a plastic drinking straw, which was rigidly fixed to the end of the sample rod. Cyclic voltammetry measurements were carried out using a Bioanalytical System BAS-100 instrument with a three-electrode cell equipped with a glassy carbon working electrode, a platinum wire auxiliary electrode and a Ag–AgCl (3 mol dm^{-3} NaCl) reference electrode. Potentials are given with respect to the ferrocene–ferrocenium couple (0.572 V *vs.* Ag–AgCl). All measurements were recorded at room temperature in dry, degassed dimethylformamide [$\approx$(1–2) × 10^{-3} mol dm^{-3}] with tetrabutylammonium perchlorate ($\approx$0.1 mol dm^{-3}) as the supporting electrolyte and a trace of ferrocene as an internal standard. Scan rates between 50 and 1000 mV s^{-1} were generally employed, the most common being 100 mV s^{-1}. Proton NMR spectra were measured on Bruker AC200 and AM300 instruments with tetramethylsilane as internal calibrant. Abbreviations used: s = singlet; d = doublet; t = triplet; m = multiplet; br = broad; ex = exchangeable on D_2O addition. Carbon-13 NMR spectra were recorded with a Bruker AC200 spectrometer using $SiMe_4$ as the internal calibrant and were broad-band decoupled. Mass spectra were recorded on a VG Micromass 7070F spectrometer.

Crystallography.—Intensity data for a red crystal of $[Ni_2L(pz)]$ (0.05 × 0.08 × 0.23 mm) were measured at room temperature on a Rigaku AFC6R diffractometer with Mo-Kα radiation (λ = 0.710 73 Å). A total of 3408 independent data (ω–2θ scan technique, $2\theta_{max}$ 50.0°) were corrected for Lorentz and polarization effects[21] and for absorption employing an empirical method[22] (range of transmission coefficients 0.892–1.042).

Crystal data. $C_{18}H_{20}N_4Ni_2O_3$, M = 457.8, triclinic, space group $P\bar{1}$, a = 9.084(2), b = 12.185(4), c = 8.269(1) Å, α = 98.01(2), β = 100.55(1), γ = 99.03(2)°, U = 875.2(3) Å^3, D_c = 1.734 g cm^{-3}, Z = 2, $F(000)$ = 472, μ = 21.79 cm^{-1}, 1283 data with $I \geqslant 3.0\sigma(I)$.

The structure was solved by direct methods[23] and refined by a full-matrix least-squares procedure based on F.[21] The non-hydrogen atoms were refined anisotropically and H atoms were included in the model at calculated positions (C–H 0.97 Å). The refinement on 244 parameters converged with R = 0.087 and R' = 0.077 (sigma weights). The maximum and minimum excursions in the final difference map were 0.89 and −0.91 e Å^{-3}, respectively. The analysis reported here is the better of two independent determinations (the other conducted at 100 K) and although it has resulted in a relatively high residual it determines the structure to be $[Ni_2L(pz)]$. Fractional atomic coordinates are listed in Table 1 and the numbering scheme employed is shown in Fig. 5 drawn with the ORTEP program using 35% probability ellipsoids.[24] Scattering factors for all atoms were as incorporated in the TEXSAN[21] package installed on an Iris Indigo workstation.

Additional material available from the Cambridge Crystallographic Data Centre comprises H-atom coordinates, thermal parameters, and remaining bond lengths and angles.

Results and Discussion

Synthesis and Characterization.—As in the synthesis of related unsymmetrical tetradentate ligands, based on a 1,2-diaminoethane backbone,[25–28] the key intermediate required to make the present pentadentate ligand, H_3L, is the 1:1 condensation product formed between acetylacetone and 1,3-diaminopropan-2-ol (see structure **I**). This was best made in chloroform as solvent and obtained as a yellow oil which was then treated quickly with salicylaldehyde in methanol as solvent to give yellow crystals of H_3L in high yield. Binuclear μ-pyrazolato complexes of the type $[M_2L(pz)]$ were obtained by treating the metal perchlorate salts (M = Ni or Cu) with H_3L and pyrazole in methanol in the presence of KOH. The complexes are stable in solution over long periods and there is no evidence for scrambling of the end groups to form symmetrical complexes.[29] The diamagnetic behaviour of $[Ni_2L(pz)]$, together with its well resolved ^1H and ^{13}C NMR spectra, the latter showing eighteen different carbon nuclei, are indicative of planar geometry around each nickel(II) ion. Similar behaviour was observed for the binuclear nickel complexes of the analogous symmetrical ligands.[30] A d–d band at 569 nm in the visible spectrum of the violet $[Cu_2L(pz)]$ complex is also indicative of planar geometry around each Cu^{II}. The magnetic moment, per Cu, of 1.33 μ_B arises from medium-strength antiferromagnetic coupling and confirms the anticipated binuclear structure of the complex in which the copper(II) ions are bridged by alkoxo and pyrazolato groups. X-Ray diffractograms taken on powders of the $[Ni_2L(pz)]$ and $[Cu_2L(pz)]$ complexes show that they are not isostructural even though their physical properties indicate that they have similar molecular structures. The crystal structure of the nickel complex is described below and confirms the planar geometry around the nickel atoms.

Table 1 Fractional atomic coordinates for $[Ni_2L(pz)]$

Atom	x	y	z
Ni(1)	0.4346(3)	0.9693(3)	0.2869(3)
Ni(2)	0.6093(3)	0.7669(2)	0.1955(3)
O(1)	0.6214(16)	0.6181(11)	0.1741(17)
O(2)	0.5822(14)	0.9149(12)	0.2031(17)
O(3)	0.2749(15)	1.0205(13)	0.3608(15)
N(1)	0.7868(18)	0.8138(18)	0.1265(20)
N(2)	0.5333(18)	1.1038(13)	0.2484(17)
N(3)	0.3568(16)	0.8235(11)	0.3190(16)
N(4)	0.4293(18)	0.7418(16)	0.2772(23)
C(1)	0.7270(26)	0.4580(20)	0.1484(32)
C(2)	0.7320(28)	0.5746(19)	0.1376(25)
C(3)	0.8541(24)	0.6338(19)	0.0876(25)
C(4)	0.8688(24)	0.7447(20)	0.0775(25)
C(5)	1.0109(25)	0.8016(21)	0.0131(31)
C(6)	0.8107(22)	0.9351(17)	0.1189(24)
C(7)	0.7098(23)	0.9818(20)	0.2189(26)
C(8)	0.6718(23)	1.0966(16)	0.1824(27)
C(9)	0.4844(25)	1.1929(25)	0.2670(27)
C(10)	0.3499(24)	1.2067(19)	0.3239(25)
C(11)	0.3293(26)	1.3268(18)	0.3474(31)
C(12)	0.2020(27)	1.3475(15)	0.4068(31)
C(13)	0.1117(24)	1.2636(20)	0.4494(29)
C(14)	0.1300(21)	1.1511(15)	0.4330(22)
C(15)	0.2594(22)	1.1255(20)	0.3701(22)
C(16)	0.2402(23)	0.7815(19)	0.3770(24)
C(17)	0.2265(22)	0.6662(19)	0.3661(29)
C(18)	0.3520(26)	0.6452(18)	0.3013(29)

Electrochemistry in Dimethylformamide Solutions.—Since the redox properties of binuclear Cu_2 and Ni_2 compounds are of particular interest from the mechanistic and bioinorganic chemical points of view,[6,8,30–32] cyclic voltammetry (CV) and Osteryoung square-wave voltammetric studies were made on dimethylformamide (dmf) solutions of the present complexes at a glassy carbon working electrode. Cyclic voltammetric data have previously been reported on the related symmetrical complexes,[30] and so it is of additional interest to try and identify which 'end' of the present unsymmetrical complex is reduced first in one-electron reductive processes. In the case of $[Ni_2L(pz)]$, CV waves are observed due to the two primary reduction processes, 1 and 2. These are shown in Fig. 1. They correspond to the following sequential one-electron steps (1) and (2). There are other weaker secondary waves of uncertain

$$[Ni_2L(pz)] + e^- \rightleftharpoons [Ni_2L(pz)]^- \qquad (1)$$

$$[Ni_2L(pz)]^- + e^- \rightleftharpoons [Ni_2L(pz)]^{2-} \qquad (2)$$

origin, described below. Similar voltammograms were observed using a platinum-button electrode. The reduction wave corresponding to (1) occurs at $E_{\frac{1}{2}}$ = −2.11 V (relative to ferrocenium–ferrocene) and has characteristics of an electrochemically reversible couple, *viz*. i_{p_a}/i_{p_c} = 1.0 and ΔE_p = 94 mV at a scan rate of 100 mV s^{-1} (N.B. ΔE_p for ferrocene under these conditions is 90 mV). A second wave occurs at more negative potentials, $E_{\frac{1}{2}}$ *ca*. −2.75 V, corresponding to process (2). It has a well defined cathodic peak but a poorly defined anodic peak. Similar CV waves are displayed by the μ-3,5-dimethylpyrazolate-bridged nickel complex (Fig. 2), although this

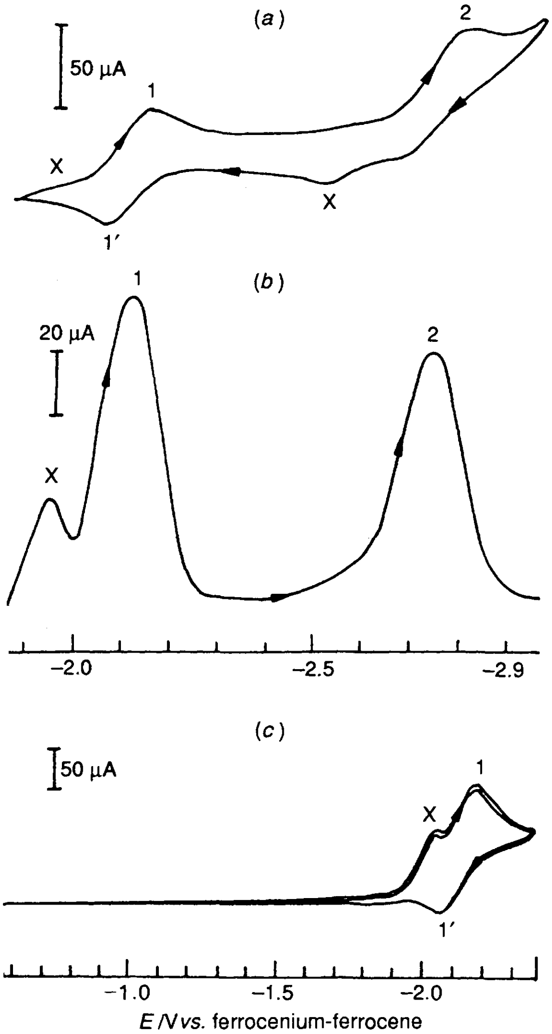

Fig. 1 Cyclic voltammograms for the reduction of 10^{-3} mol dm^{-3} $[\mathrm{Ni_2L(pz)}]$ in dmf at 20 °C using a scan rate of 100 mV s^{-1}, a glassy carbon electrode and supporting electrolyte 0.1 mol dm^{-3} $\mathrm{NBu_4ClO_4}$. (*a*) Voltage range −1.80 to −2.90 V showing primary waves 1 and 2 and secondary waves, X; (*b*) Osteryoung square-wave voltammogram corresponding to (*a*); (*c*) voltage range −0.57 to −2.30 V showing five cycles

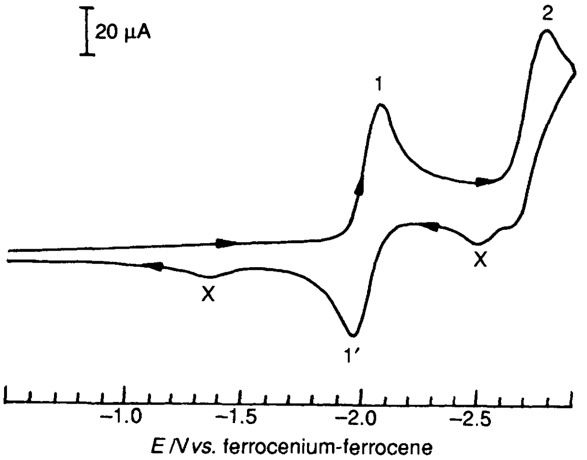

Fig. 2 Cyclic voltammogram for the reduction of 10^{-3} mol dm^{-3} $[\mathrm{Ni_2L(dmpz)}]$ in dmf at 20 °C using a scan rate of 100 mV s^{-1}, a glassy carbon electrode and 0.1 mol dm^{-3} $\mathrm{NBu_4ClO_4}$ as supporting electrolyte

complex is somewhat easier to reduce with an $E_{\frac{1}{2}}$ value for process (1) of −2.02 V. The relative ease of reduction of the μ-3,5-dimethylpyrazolate compound compared to the pyrazole derivative was also noted within the symmetrical complex analogues.[30] The $E_{\frac{1}{2}}$ value for process (1) in the $[\mathrm{Ni_2L(pz)}]$ complex is similar in size to that for the analogous *N,N′*-bis(salicylidene) complex, the latter having[30] $E_{\frac{1}{2}} = -2.06$ V, whilst the cathodic peak for process (2), with $E_{p_c} = -2.81$ V, occurs at a similar potential to that for the *N,N′*-bis(1-methyl-3-oxobut-1-enyl) complex, *viz.* $E_{p_c} = -2.84$ V. The data in ref. 30 were corrected to the ferrocene scale by adding −0.49 V. If it is assumed that the first electron remains localized on one of the nickel ions for the duration of the CV time-scale, prior to the second reduction process taking place, then these comparative data suggest that the first electron transfer occurs at the nickel(II)–salicylidene end of the molecule whilst the second occurs at the nickel(II)–1-methyl-3-oxobutenyl moiety.

In a somewhat related way to that noted by Bond and co-workers[30] in CV studies on symmetrical analogues of the present complex and on related μ-phenolato-μ-pyrazolato complexes,[2,31] there are minor waves due to secondary processes in the $[\mathrm{Ni_2L(pz)}]$ systems. These are marked X in Figs. 1 and 2. Whilst we have not monitored these waves as a function of temperature in the way that was done previously,[30,31] it is noted that the cathodic peak at $E_{p_c} = -2.02$ V observed both by CV and square-wave techniques diminishes in the size of i_{p_c} on multiple cycles from cycle 1 to 5. It is distinctive when starting the cathodic sweeps from a potential of −0.57 V, but barely observable when starting the sweep at −1.90 V. This additional cathodic peak is not present on the first reduction wave of $[\mathrm{Ni_2L(dmpz)}]$. The latter complex does show a minor anodic wave at $E_{p_a} = -2.49$ V, as does $[\mathrm{Ni_2L(pz)}]$, which, by square-wave measurements, is confirmed not to be the anodic component of the primary process (2) and is more prominent when sweeping anodically from very negative potentials such as −2.90 V, than it is when sweeping cathodically from −1.80 V. Thus, the occurrence and life of these minor waves are dependent on time and on starting voltage which presumably means that secondary electroactive species are present or are being generated. There is, however, no direct evidence for the presence of minor species from analytical or spectroscopic data. We have not measured ESR spectra on the $[\mathrm{Ni_2L(pz)}]^-$ species to try and identify the presence of more than one reduced form.[30] Axial solvation by dmf molecules does not occur here, this being the reason for similar minor processes being noted in the CV of related μ-phenolato-μ-pyrazolato complexes.[2,31] The most likely explanation is that given by Bond and co-workers[30] for the symmetrical analogues of $[\mathrm{Ni_2L(pz)}]$ and $[\mathrm{Ni_2L(dmpz)}]$, *i.e.* the presence of two closely related structural forms.

The CV scans measured on the complex $[\mathrm{Cu_2L(pz)}]$, under similar conditions to those used for the nickel analogue, reveal a quasi-reversible reduction process at $E_{\frac{1}{2}} = -1.51$ V with a $\Delta E_p = 120$ mV and $i_{p_a}/i_{p_c} = 0.8$. Fig. 3 shows that a broad irreversible reduction process also occurs at *ca.* −2.23 V. The data are generally similar to those displayed by the nickel compound, the first wave being due to process (1). The half-wave potential for this first process compares to an $E_{\frac{1}{2}}$ value of −1.52 V and $\Delta E_p = 257$ mV for the similarly behaved symmetrical *N,N′*-bis(salicylidene) complex, determined at a platinum electrode. The only comparative data on a symmetrical *N,N′*-bis(1-methyl-3-oxobut-1-enyl) complex of copper (II) also determined at platinum electrode, was for the compound containing a μ-3,5-dimethylpyrazolate bridging group, which showed $E_{\frac{1}{2}} = -1.59$ V. It has been observed previously[30] that the reduction of dimethylpyrazolate-bridged species are easier relative to that of the pyrazolate analogues by some 0.1 V. This behaviour again has been noted in the current study and, thus, the reduction of the pyrazolato-bridged symmetrical *N,N′*-bis(1-methyl-3-oxobutenyl) complex would be expected to occur at potentials lower than −1.59 V. The CV data on the copper complexes also, therefore, support the

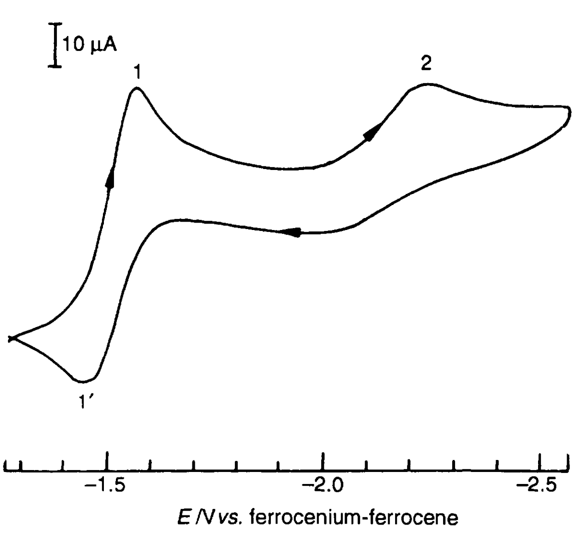

Fig. 3 Cyclic voltammogram for the reduction of 10^{-3} mol dm^{-3} $[Cu_2L(pz)]$ in dmf at 20 °C using a scan rate of 100 mV s^{-1}, a glassy carbon electrode and 0.1 mol dm^{-3} NBu_4ClO_4 as supporting electrolyte

postulate that the first reduction process occurs at the copper(II)–salicylidene end of the binuclear molecule.

Apart from the subtleties described above, the CV data for the $[Ni_2L(pz)]$, $[Ni_2L(dmpz)]$ and $[Cu_2L(pz)]$ species are generally similar to those reported for the symmetrical relatives.[30] Thus, it seems likely that the redox cross-reaction (3)

$$[Cu_2L(pz)]^{2-} + [Cu_2L(pz)] \rightleftharpoons 2[Cu_2L(pz)]^{-} \quad (3)$$

and the possible existence of structurally different binuclear forms[30] are relevant to the present unsymmetrical species. Finally, it is clear that the incorporation of structurally different ends to the binuclear molecules does not increase the electrochemical complexity compared to the situation in which the ends are symmetrical.

Crystal Structure of $[Ni_2L(pz)]$.—The crystal structure of $[Ni_2L(pz)]$ is of relatively low precision (see Experimental section), however the molecular structure has been determined unambiguously. The molecular structure is shown in Fig. 4 and selected interatomic parameters are collected in Table 2. The Ni atoms in the dinuclear structure are linked symmetrically by the pyrazole group [Ni(1)–N(3) 1.88(1) and Ni(2)–N(4) 1.88(2) Å]. The two Ni–O(2) distances of 1.79(1) and 1.85(1) Å tend to suggest some asymmetry in the alkoxide bridge, however we note the relatively high errors associated with these parameters which preclude a definitive conclusion. The remaining sites in the square-planar nickel geometries are occupied by phenoxide O(3) and imino N(2) atoms for the Ni(1) atom and for the Ni(2) centre by the alkoxide O(1) atom and imino N(1) atom. Thus, each Ni atom exists in *trans*-N_2O_2 geometry. The mean deviation from the least-squares plane through the $Ni(1)N_2O_2$ atoms is 0.028 Å and the equivalent value for the Ni(2) plane is 0.044 Å; the dihedral angle between the two planes is 177.6°. The dihedral angle for the symmetrical bis(salicylidene) analogue[32] is 179.1°. Whereas the mean deviation from the Ni(1)Ni(2)O(2)N(3)N(4) plane is 0.023 Å, the other five-membered rings are not planar as seen in the values for the O(2)–C(7)–C(8)–N(2) and O(2)–C(7)–C(6)–N(1) torsion angles of 34(2) and −37(2)°, respectively. The two remaining six-membered rings are each planar to ±0.06(2) Å. The Ni(1) ··· Ni(2) separation within the molecule is 3.212(4) Å. In the lattice the essentially planar molecules lie in the crystallographic *ab* plane and are stacked along the *c* axis so that the separation between adjacent layers is approximately 3.5 Å; a view of the unit-cell contents is shown in Fig. 5. Of note is a Ni(1) ··· Ni(1′) separation of 3.442(5) Å which occurs between centrosymmetrically related (symmetry operation: 1 − *x*, 2 − *y*, 1 − *z*) pairs of molecules; the Ni(2) ··· Ni(2′) separation is 5.100(4) Å. These intermolecular contacts are important in fully describing the magnetic data for the $[Cu_2L(pz)]$ complex, as indicated below.

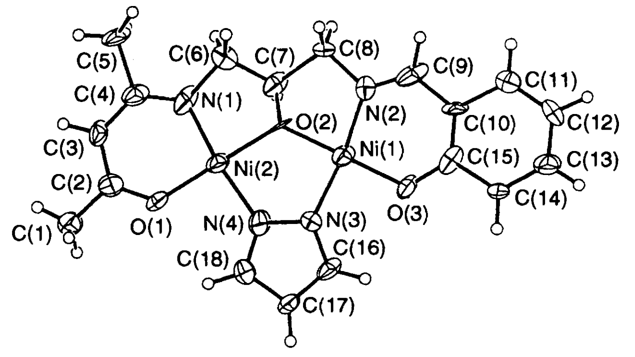

Fig. 4 Molecular structure and numbering scheme of $[Ni_2L(pz)]$ drawn with the ORTEP[24] program using 35% probability ellipsoids

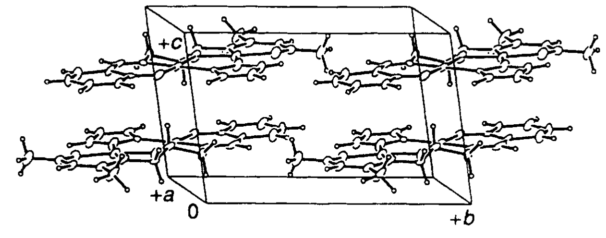

Fig. 5 Unit-cell contents of $[Ni_2L(pz)]$

Table 2 Selected bond distances (Å) and angles (°) for $[Ni_2L(pz)]$

Ni(1)–O(2)	1.79(1)	Ni(1)–O(3)	1.84(1)
Ni(1)–N(2)	1.84(1)	Ni(1)–N(3)	1.88(1)
Ni(2)–O(1)	1.82(1)	Ni(2)–O(2)	1.85(1)
Ni(2)–N(1)	1.84(2)	Ni(2)–N(4)	1.88(2)
O(2)–Ni(1)–O(3)	176.5(7)	O(2)–Ni(1)–N(2)	83.0(6)
O(2)–Ni(1)–N(3)	89.2(6)	O(3)–Ni(1)–N(2)	98.2(6)
O(3)–Ni(1)–N(3)	89.7(6)	N(2)–Ni(1)–N(3)	172.1(6)
O(1)–Ni(2)–O(2)	175.1(7)	O(1)–Ni(2)–N(1)	96.4(7)
O(1)–Ni(2)–N(4)	91.8(7)	O(2)–Ni(2)–N(1)	85.7(7)
O(2)–Ni(2)–N(4)	86.3(6)	N(1)–Ni(2)–N(4)	171.5(9)
Ni(1)–O(2)–Ni(2)	123.7(6)		

Magnetic Exchange in the Complex $[Cu_2L(pz)]$.—The plot of magnetic susceptibility *versus* temperature for $[Cu_2L(pz)]$, given in Fig. 6, shows a broad maximum at a temperature of *ca.* 230 K indicative of an antiferromagnetically coupled system. A small amount of monomer impurity (0.1%) is responsible for the increase in susceptibility below 10 K. The corresponding magnetic moment values are 1.33 μ_B (per Cu) at 295 K and 0.05 μ_B at 4.2 K. In attempting to fit the χ *vs.* T data it was found that a two-J tetranuclear model,[33,34] similar to that used for the symmetrical *N,N′*-bis(salicylidene) and *N,N′*-bis(2-pyridylmethylene) complexes containing μ-OH or μ-Cl exogenous bridges,[10] was superior to a simple one-J binuclear model. Thus an excellent fit to the data was obtained for the following parameter values: $g = 1.92$, $N\alpha = 7.54 \times 10^{-10}$ m^3 mol^{-1}, $J_{12} = -129$ cm^{-1}, $J_{\text{intermol}} = -41$ cm^{-1}. The exchange-coupling constants for the symmetrical copper(II) complexes are, for comparison: *N,N′*-bis(salicylidene), $J_{12} = -120$ cm^{-1}, $J_{\text{intermol}} = 0$; *N,N′*-bis(1-methyl-3-oxobut-1-enyl), $J_{12} = -100$ cm^{-1}, $J_{\text{intermol}} = 0$. The value quoted for the *N,N′*-bis(salicylidene) complex is for a sample which contained one molecule of

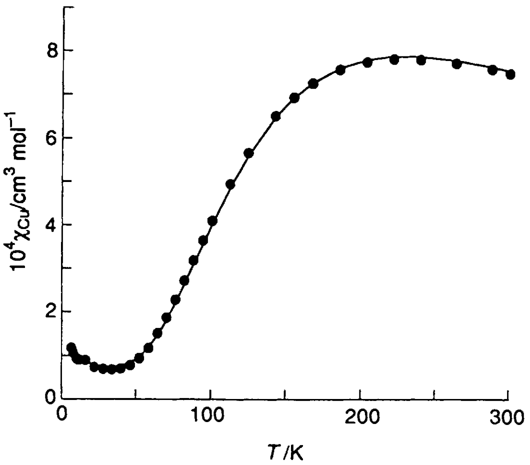

Fig. 6 Plot of magnetic susceptibility, per Cu, *versus* temperature for [Cu$_2$L(pz)] in an applied field of 1 T. The solid line is the best-fit calculated curve using the parameters $g = 1.92$, $N\alpha = 7.54 \times 10^{-10}$ m^3 mol^{-1}, $J_{12} = -129$ cm^{-1}, $J_{\text{intermol}} = -41$ cm^{-1}

co-ordinated water.[11] A structurally similar anhydrous form was reported by Nishida and Kida[35] to show a best-fit J_{12} value of -155 cm^{-1}, with no allowance being made in the fitting for an intermolecular Cu ··· Cu contact of 4.2 Å. In this kind of doubly bridged μ-pyrazolato-μ-alkoxo framework, based on the 1,3-diaminopropan-2-olato backbone,[11,13,35] the J values lie in a confined range of $-(100$ to $150)$ cm^{-1}. Our previous work,[11] and that done more recently by using the more flexible backbone systems based on 1,5-diaminopentan-3-ol and 1,4-diaminobutan-2-ol, show larger negative J values *i.e.* > -270 cm^{-1}. These variations in J have been ascribed to the complementary (large J) or countercomplementary (smaller J) effect of the pyrazolate-bridge overlap on the alkoxo-bridge overlap in determining the overall size of the exchange coupling.[13,35] These, and related arguments by Reed *et al.*[5] and Kahn,[36] are subtle and persuasive when comparing closely related doubly bridged systems of the present type. Nevertheless, further testing of these ideas needs to be done on structurally characterized compounds. Our own work has shown, for instance, that when the bridging framework is kept constant, but the end groups are varied, large changes in J can ensue.[10,11]

We are presently extending the co-ordination chemistry of compound H$_3$L to mixed-metal species. New unsymmetrical ligands, with different end-groups, are being developed from the intermediate **I**. Tetranuclear complexes of type [(M$_2$L)$_2$L′] [L′ = 4,4′-di(3,5-dimethylpyrazolate)] have also been synthesized for comparison with recently reported analogues which contain a double-pyrazolate spacer (L′).[37] Unusual combinations of four different metal ions are possible in such systems. Two papers dealing with unsymmetrical ligands and using structural principles related to those used here have just appeared.[38]

Acknowledgements

The Australian Research Council (ARC) is thanked for support of the crystallographic facility at the University of Adelaide and for ARC grants (to K. S. M.) and an Australian Postdoctoral Fellowship (to B. M.).

References

1 D. E. Fenton and H. Okawa, *J. Chem. Soc., Dalton Trans.*, 1993, 1349; P. Guerriero, P. A. Vigato, D. E. Fenton and P. C. Hellier, *Acta Chem. Scand.*, 1992, **46**, 1025.
2 A. M. Bond, M. Haga, I. S. Creece, R. Robson and J. C. Wilson, *Inorg. Chem.*, 1989, **28**, 559.
3 O. Kahn, *Struct. Bonding (Berlin)*, 1987, **68**, 89.
4 S. S. Tandon, L. K. Thompson and J. N. Bridson, *J. Chem. Soc., Chem. Commun.*, 1993, 804.
5 C. A. Reed, *Research Frontiers in Magnetochemistry*, ed. C. J. O'Connor, World Scientific Publishing Co., Singapore, New Jersey, London, Hong Kong, 1993, p. 351.
6 K. D. Karlin and Z. Tyeklar (Editors), *Bioinorganic Chemistry of Copper*, Chapman and Hall, New York, 1993.
7 L. Que, jun., and A. E. True, *Prog. Inorg. Chem.*, 1990, **38**, 97.
8 R. Das and K. Nag, *Inorg. Chem.*, 1991, **30**, 2831.
9 N. A. Bailey, K. C. Cox, C. P. Falshaw, D. E. Fenton, S. E. Grundy, P. Hough, C. A. Phillips and T. J. King, *J. Chem. Soc., Dalton Trans.*, 1983, 224.
10 W. Mazurek, K. J. Berry, K. S. Murray, M. J. O'Connor, M. R. Snow and A. G. Wedd, *Inorg. Chem.*, 1982, **21**, 3071.
11 W. Mazurek, K. J. Berry, K. S. Murray, M. J. O'Connor, J. R. Rodgers, M. R. Snow, A. G. Wedd and P. R. Zwack, *Inorg. Chem.*, 1985, **24**, 3528.
12 M. S. Nasir, K. D. Karlin, D. McGowty and J. Zubieta, *J. Am. Chem. Soc.*, 1991, **113**, 698.
13 T. N. Doman, D. E. Williams, J. F. Banks, R. M. Buchanan, H.-R. Chang, R. J. Webb and D. N. Hendrickson, *Inorg. Chem.*, 1990, **29**, 1058.
14 L. L. Borer and E. Sinn, *Inorg. Chim. Acta*, 1988, **142**, 197.
15 P. Kamaras, M. C. Cajulis, M. Rapta and G. B. Jameson, *J. Inorg. Biochem.*, 1993, **51**, 186.
16 R. M. Buchanan, *J. Inorg. Biochem.*, 1993, **51**, 444.
17 G. D. Fallon, A. Markiewicz, K. S. Murray and T. Quach, *J. Chem. Soc., Chem. Commun.*, 1991, 198.
18 R. C. Holtz, T. E. Elgren, L. L. Pearce, J. H. Zhang, C. J. O'Connor and L. Que, jun., *Inorg. Chem.*, 1993, **32**, 5844.
19 M. Osawa, U. P. Singh, M. Tanaka, Y. Moro-Oka and N. Kitajima, *J. Chem. Soc., Chem. Commun.*, 1993, 310.
20 P. Gomez-Romero, E. A. Witten, M. W. Reiff, G. Backer, J. Sanders-Loehr and G. B. Jameson, *J. Am. Chem. Soc.*, 1989, **111**, 9039.
21 TEXSAN, Structure Analysis Package, Molecular Structure Corporation, Houston, TX, 1992.
22 N. Walker and D. Stuart, *Acta Crystallogr., Sect. A*, 1983, **39**, 158.
23 H.-F. Fan, SAPI91, Structure Analysis Package with Intelligent Control, Rigaku Corporation, Tokyo, 1991.
24 C. K. Johnson, ORTEP II, ORNL Report 4136, Oak Ridge National Laboratory, Oak Ridge, TN, 1976.
25 J.-P. Costes, *Bull. Soc. Chim. Fr.*, 1986, 78.
26 J.-P. Costes, G. Cros, M. H. Darbieu and J.-P. Laurent, *Inorg. Chim. Acta*, 1982, **60**, 111.
27 A. Garcia-Deibe, M. R. Bermejo, A. Sousa, C. A. McAuliffe, P. McGlynn, P. T. Ndifon and R. G. Pritchard, *J. Chem. Soc., Dalton Trans.*, 1993, 1605.
28 M. Fukuya, M. Ohba, K.-I. Motoda, N. Matsumoto, H. Okawa and Y. Maeda, *J. Chem. Soc., Dalton Trans.*, 1993, 3277.
29 A. Garcia-Deibe, M. R. Bermejo, A. Sousa, P. P. MacRory, C. A. McAuliffe, R. G. Pritchard and M. Helliwell, *J. Chem. Soc., Chem. Commun.*, 1991, 728.
30 W. Mazurek, A. M. Bond, M. J. O'Connor and A. G. Wedd, *Inorg. Chem.*, 1986, **25**, 906.
31 A. M. Bond, M. A. Haga, I. S. Creece, R. Robson and J. C. Wilson, *Inorg. Chem.*, 1988, **27**, 712.
32 M. Mikuriya, T. Sasaki, A. Anjiki, S. Ikenoue and T. Tokii, *Bull. Chem. Soc. Jpn.*, 1992, **65**, 334.
33 W. E. Hatfield and G. W. Inman, *Inorg. Chem.*, 1969, **8**, 1376.
34 P. D. W. Boyd and R. L. Martin, *J. Chem. Soc., Dalton Trans.*, 1977, 105.
35 Y. Nishida and S. Kida, *Inorg. Chem.*, 1988, **27**, 447.
36 O. Kahn, *Molecular Magnetism*, VCH, New York, Weinheim, Cambridge, 1993, ch. 8, p. 164.
37 P. E. Kruger, G. D. Fallon, B. Moubaraki and K. S. Murray, *J. Chem. Soc., Chem. Commun.*, 1992, 1726.
38 C. Fraser, R. Ostrander, A. L. Rheingold, C. White and B. Bosnich, *Inorg. Chem.*, 1994, **33**, 324; C. Fraser and B. Bosnich, *Inorg. Chem.*, 1994, **33**, 338.

Received 25*th January* 1994; *Paper* 4/00469H